Chin. Phys. Lett. **39**, 037501 (2022)

Dynamic Cantilever Magnetometry of Paramagnetism with Slow Relaxation

Zhiyu Ma(马知雨)[1,2], Kun Fan(樊坤)[3], Qi Li(李奇)[1,2], Feng Xu(徐峰)[1], Lvkuan Zou(邹吕宽)[1*], Ning Wang(王宁)[1], Li-Min Zheng(郑丽敏)[3*], and Fei Xue(薛飞)[1*]

[1]*Anhui Key Laboratory of Condensed Matter Physics at Extreme Conditions, High Magnetic Field Laboratory, Hefei Institutes of Physical Science, Chinese Academy of Sciences, Hefei 230031, China*
[2]*Science Island Branch, Graduate School, University of Science and Technology of China, Hefei 230026, China*
[3]*State Key Laboratory of Coordination Chemistry, School of Chemistry and Chemical Engineering, Nanjing University, Nanjing 210023, China*

(Received 13 December 2021; accepted 18 January 2022; published online 1 March 2022)

Dynamic cantilever magnetometry is a sensitive method that has been widely used in studying magnetic anisotropy in ferromagnetic materials and Fermi surface in quantum materials. We study a cobalt-iridium metal-metalloligand coordination polymer using dynamic cantilever magnetometry. The experimental data of dynamic cantilever magnetometry are well explained using the proposed model for Langevin paramagnetism with slow relaxation. Based on the proposed model, we calculate the magnetization and magnetic susceptibility of paramagnetic materials from frequency shifts of a cantilever. The extracted magnetization and magnetic susceptibility are consistent with those obtained from conventional DC and AC magnetometry. The proposed slow relaxation picture is probably a general model for explaining dynamic cantilever magnetometry data of paramagnetic materials, including previously observed dynamic cantilever magnetometry data of paramagnetic metals [Gysin *et al.* 2011 *Nanotechnology* **22** 285715].

DOI: 10.1088/0256-307X/39/3/037501

Dynamic cantilever magnetometry (DCM),[1,2] also known as torque differential magnetometry,[3] is an emerging technique developed in recent decades renowned by its high detection sensitivity for magnetic anisotropy[4–6] and unique resolution for micro or nanosamples.[7–9] Starting from ferromagnetic materials,[10] the scope of dynamic cantilever magnetometry has extended to quantum materials like Kondo insulator,[11] Dirac semimetal,[12] Weyl semimetal,[13] and quantum spin liquids.[14–17] These materials exhibit Landau diamagnetism at a low magnetic field, which does not contribute to magnetic torque and resonance frequency shift. Meanwhile, at high field and low temperature, quantum oscillation of physical properties like de Haas-van Alphen effect and Berry paramagnetism arising from materials' nontrivial topology dominate the behavior of magnetic torque and frequency shift. In contrast to static torque magnetometry, which directly measures magnetic torque, dynamic cantilever magnetometry is sensitive to magnetization dynamics, thereby making dynamic cantilever magnetometry an ideal method for investigating materials with slow magnetic relaxation.[18] Though magnetic anisotropy and quantum oscillation of materials using DCM have been intensively studied,[4,12,13] relaxation properties are rarely mentioned. Mechanical detection with dynamic cantilever magnetometry will provide an alternative way to study the relaxation process of magnetic materials.

Recently, tunable functionality in cobalt-based molecular materials[19–21] has made them promising candidates for miniature sensors.[22–24] Several studies have investigated the static torque magnetometry of coordination compounds.[25] In this work, we apply dynamic cantilever magnetometry to systematically study Langevin paramagnetism of a cobalt-iridium metal-metalloligand coordination polymer $[Co^{II}_3(\mu_3-O)(\mu-OH_2)\{Ir^{III}(ppy-COO)_2(ppy-COOH)\}_2(H_2O)_4]\cdot 2DMF\cdot xH_2O$.[26] The experimental results show that the coordination polymer exhibits paramagnetism with slow relaxation up to 300 K. One possible origin of this phenomenon is spin-glass caused by magnetic frustration in trimetallic units of the crystal structure.[26]

The polymer sample was synthesized using a solvothermal method and has been demonstrated to display paramagnetism down to 2 K in previous study.[26] By soaking in acetone and raising the temperature above 333 K, the material experiences single-crystal to single-crystal (SC-SC) structural transformation to the other two compounds, which will not be discussed in this work. Then, an as-grown single-crystal rod was transferred to the free end of a can-

*Corresponding authors. Email: zoulvkuan@hmfl.ac.cn; lmzheng@nju.edu.cn; xuef@hmfl.ac.cn
© 2022 Chinese Physical Society and IOP Publishing Ltd

tilever using a micro-manipulator. Figure 1 shows the experimental setup of dynamic cantilever magnetometry. The silicon cantilever used here was 500 μm long, 100 μm wide, and 1 μm thick. The resonance frequency of the cantilever was measured to be 4309 Hz using a home-built microlens fiber-optic interferometer system, which uses a 1550-nm laser with an incident power less than 1 μW. The dynamic cantilever magnetometry experiments were conducted in a vacuum chamber with a pressure below 1×10^{-6} mbar. The cylindrical crystalline sample attached at the free end of the cantilever has a diameter of 15 μm and a length of 147 μm. The magnetic field was produced from a superconducting magnet. In our experiment, the long axis of the sample and cantilever, applied magnetic field are along the y axis, as shown in Fig. 1.

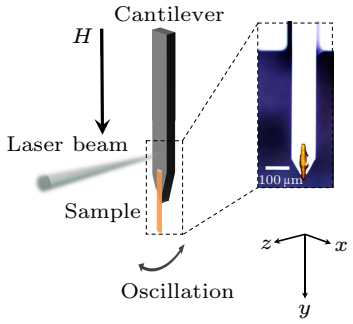

Fig. 1. Schematic of dynamic cantilever magnetometry measurement, including oscillating cantilever (dark gray), laser from the interferometer (light gray), and the polymer sample (orange). The inset shows an optical photo of an individual sample attached on the cantilever's free end.

In previous studies of dynamic cantilever magnetometry, conventional inorganic ferromagnetic materials have been intensively studied.[27–29] Generally, the relaxation of magnetization is several orders of magnitude faster than the cantilever's oscillation.[30] Thus, at every moment of the cantilever's oscillation, magnetization has already completed the relaxation process and resides to an equilibrium position between the external magnetic field and easy axis of the sample, as illustrated in Fig. 2(a). The deviation angle ϕ is calculated by minimizing the energy of the system with respect to ϕ. The total energy can be written as

$$E(\theta) = \frac{1}{2}k_0(l_e\theta)^2 - \mu_0 MVH\cos(\theta - \phi) + E_{\text{ani}}, \quad (1)$$

where the first, second, and third terms represent the cantilever, Zeeman, and effective anisotropy energies, respectively; μ_0, k_0, l_e, θ, M, and V are permeability of vacuum, inherent spring constant, effective length, oscillation angle of the cantilever, magnetization, and volume of the sample,[27] respectively. M is a constant in the single-domain assumption. Since $\theta \ll 1$, resonance frequency shift has a universal form of

$$\Delta f = \frac{f_0}{2k_0 l_e^2}\left(\frac{\partial^2 E}{\partial \theta^2} - k_0 l_e^2\right), \quad (2)$$

where f_0 is the resonance frequency in the absence of a magnetic field. The explicit expression of Δf depends on the type of magnetic anisotropy E_{ani}. Uniaxial anisotropy is almost the only form that can give an analytical function of the magnetic field yet discovered. In our recent study,[4] we successfully extracted a hybrid magnetic anisotropy consisting of a cubic and uniaxial anisotropy in a non-analytical way.

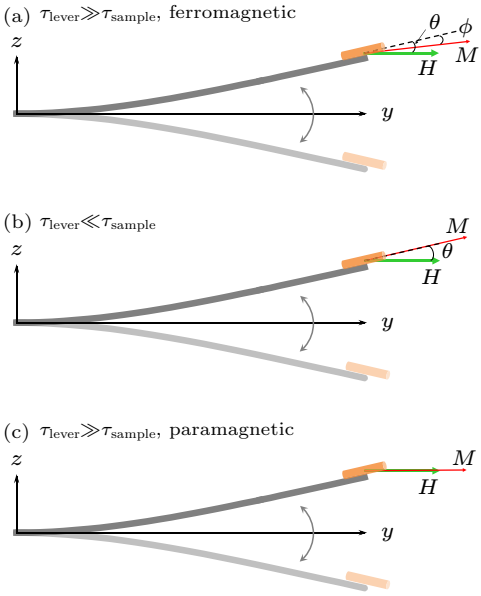

Fig. 2. Schematic view of the relative orientations of the cantilever axis, applied magnetic field $\boldsymbol{H}$, and magnetization $\boldsymbol{M}$ in dynamic cantilever magnetometry (a) for ferromagnetic material with relaxation time τ_{sample} much smaller than the cantilever's oscillation period τ_{lever}, (b) for ferromagnetic material with relaxation time τ_{sample} much longer than the cantilever's oscillation period τ_{lever}, and (c) for paramagnetic material with relaxation time τ_{sample} much smaller than the cantilever's oscillation period τ_{lever}. Here θ is the cantilever's oscillation angle, and ϕ indicates the deviation of $\boldsymbol{M}$ from the easy axis of the ferromagnetic material.

However, the situation is quite different for metal-metalloligand coordination polymer studied in this work because magnetic relaxation time is much longer than the cantilever's oscillation period, resulting in a picture that magnetization cannot catch up with the change in the external magnetic field as if the magnetization is frozen at the cantilever's free end, as shown in Fig. 2(b). Then, the total energy can be simply expressed as

$$E(\theta) = \frac{1}{2}k_0(l_e\theta)^2 - \mu_0 MVH\cos\theta. \quad (3)$$

Substituting it into Eq. (2), we have

$$\Delta f = \frac{f_0}{2k_0 l_e^2}\mu_0 MVH. \quad (4)$$

At a high magnetic field that magnetization reaches saturation, frequency shift varies proportionally with the magnetic field. This linear dependence

also occurs in permanent magnets like Sm–Co alloy and $Nd_2Fe_{14}B$.

Figure 2(c) shows another model where the relaxation of a paramagnetic material is much faster than the cantilever's oscillation. In this figure, no magnetic torque exists; thus, the measured frequency shift shows no dependence on the magnetic field. We conducted dynamic cantilever magnetometry measurements on a platinum film that has fast relaxation with the same setup, as shown in Fig. 1. As expected, in Fig. 3(a), no frequency shift was observed up to 1 T.

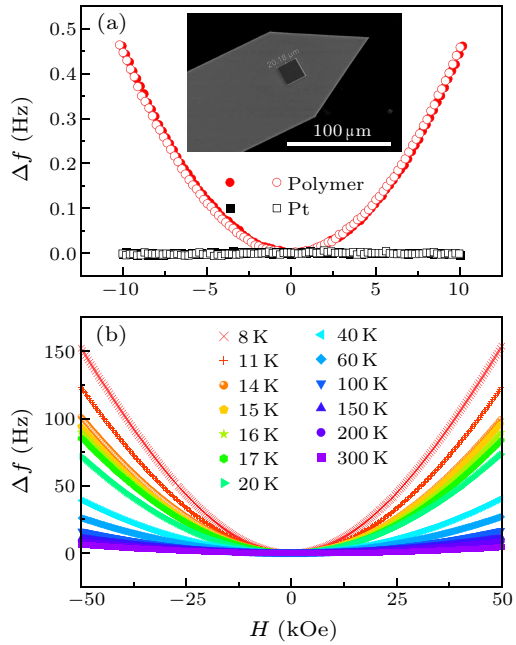

Fig. 3. (a) Representative experimental result measured at 150 K. For coordination polymer studied here, no hysteresis can be recognized in the curves of Δf vs H, indicating the absence of ferromagnetic or ferrimagnetic ordering in the material. Fittings show well quadratic dependence of frequency shift on the magnetic field. As a control sample, the frequency of Pt changes relatively little, which is on the same order of magnitude as the background noise. (b) Measured field dependence of frequency shift in dynamic cantilever magnetometry at temperatures 8 K–300 K. Here, Δf shows well quadratic dependence of H at a low field but tends to deviate from the relation at a large field as the temperature decreases.

To evaluate the model derived above, we choose the cobalt-iridium metal-metalloligand coordination polymer sample for experiments. Figure 3(a) shows the measured temperature dependence of Δf on magnetic field H. A quadratic function $\Delta f \propto H^2$ occurs at low fields. The coefficient increases with the falling temperature. This relation has also been reported in paramagnetic Dy and Gd.[1] At low temperature and large field regions, Δf vs H tends to deviate from the parabolic form, which can be identified from the first derivative of Δf with respect to H in Fig. 4(a). In fact, $\partial f/\partial H$ vs H can be well fitted by the Langevin function. Figure 4(b) shows the plot for temperature dependence of the linear part slope in $\partial f/\partial H$ vs H at low field to check whether $\partial f/\partial H$ reflects magnetization of a paramagnetic material. We obtain that $\partial^2 f/\partial H^2$ is inversely proportional to the deviation of the temperature T from a constant Θ_a, as expressed by

$$\frac{\partial^2 f}{\partial H^2} = \frac{C}{T - \Theta_a}, \tag{5}$$

which has the same form as the Curie–Weiss law.

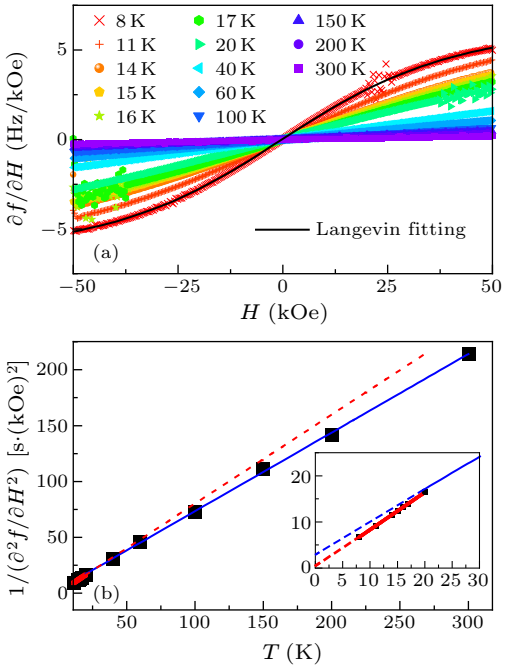

Fig. 4. (a) Field dependence of $\partial f/\partial H$ at temperatures 8 K–300 K. Data at 8 K can be well fitted by the Langevin function (black line), as expressed by Eq. (7). (b) Temperature dependence of $\partial^2 f/\partial H^2$ that obeys the Curie–Weiss law. It demonstrates that the measured $\partial^2 f/\partial H^2$ is proportional to the initial susceptibility of the sample. The inset shows the deviation of the fitted slope around 20 K, indicating a transition of intramolecular coupling.

This can be well explained using the slow relaxation model. From Eq. (4), we have

$$\frac{\partial f}{\partial H} = \frac{f_0 V \mu_0}{2k_0 l_e^2}\left[M(H) + H\frac{dM(H)}{dH}\right]. \tag{6}$$

Here, M is a Langevin function of the magnetic field H. In linear part of M vs H at low field, the relation reduces to

$$\frac{\partial f}{\partial H} = \frac{f_0 V \mu_0}{k_0 l_e^2} M(H). \tag{7}$$

The magnetic susceptibility almost approaches zero for the region where the magnetization reaches saturation when a field is sufficiently high. Thus, we have

$$\frac{\partial f}{\partial H} \approx \frac{f_0 V \mu_0}{2k_0 l_e^2} M(H). \tag{8}$$

This explains why $\partial f/\partial H$ in Fig. 4(a) can be fitted by the Langevin function. The difference between the

coefficient in Eqs. (7) and (8) requires a high magnetic field, which is beyond the measurement capability of our instrument.

By this way, the initial susceptibility at low field can be obtained from the second derivative of frequency shift with respect to field,

$$\frac{\partial^2 f}{\partial H^2} = \frac{f_0 V \mu_0}{k_0 l_e^2} \chi. \tag{9}$$

This relation helps to understand the Curie–Weiss law in Eq. (5). The positive intercept fitted in the experiment shows that the constant Θ_a is an asymptotic Curie point, i.e., $\Theta_a < 0$, implying an antiferromagnetic coupling below the Néel point. From Curie constant C, we calculate the effective atomic moment as $0.69\mu_B$, which is slightly smaller than the typical value of one cobalt. This can be mainly attributed to the antiferromagnetic coupling between the Co centers. It is worth noting that the fitted slope in $1/(\partial^2 f/\partial H^2)$ vs T shows a deviation at 20 K, as shown in the inset in Fig. 4(b). This indicates a change in absolute saturation magnetization represented by the constant C, implying a transition of intramolecular coupling.

Figure 5 shows the quantitative result of magnetization and susceptibility of the polymer material based on our slow relaxation model. The parameters obtained by dynamic cantilever magnetometry are consistent with that of the previous study, as shown by the red circle in Fig. 5(b) (see Fig. S9 in the Supporting Information of Ref. [26]). The discrepancy between the DCM and the superconducting quantum interference device probably comes from the inaccuracy in determining values k_0, l_e, and V. The comb-like pattern in Fig. 5(a) and some dispersion data in Fig. 4(a) come from instrument noise. Compared with conventional techniques like DC and AC magnetometry, diverse cantilevers ranging from nanowires to macroscopic structures induce dynamic cantilever magnetometry with high dynamic range, almost covering the entire spectrum of DC, AC magnetometry, and nuclear magnetic resonance. The advantage of our model originates from the broad frequency range and high sensitivity of dynamic cantilever magnetometry.

One possible origin of slow relaxation up to room temperature in the material is frustration-induced spin-glass behavior,[31] as mentioned in our previous study.[26] The trimeric Co_3O secondary building unit in the polymer crystal provides a structural foundation for the magnetic frustration since antiferromagnetic coupling exists between Co centers. The degree of frustration, quantified by $f = |\Theta|/T_C$, where Θ and T_C are the asymptotic Curie and Néel points, respectively, suggests a well geometric spin frustration.[26]

The proposed slow relaxation model can account for the observed $\Delta f \propto H^2$ relation in various materials. Based on these experiments, we believe that the observed dynamic cantilever magnetometry data of paramagnetic Dy and Gd and coordination polymer in this study originate from the same physics. Our proposed slow relaxation model is probably a general description of Langevin paramagnetic dynamic cantilever magnetometry.

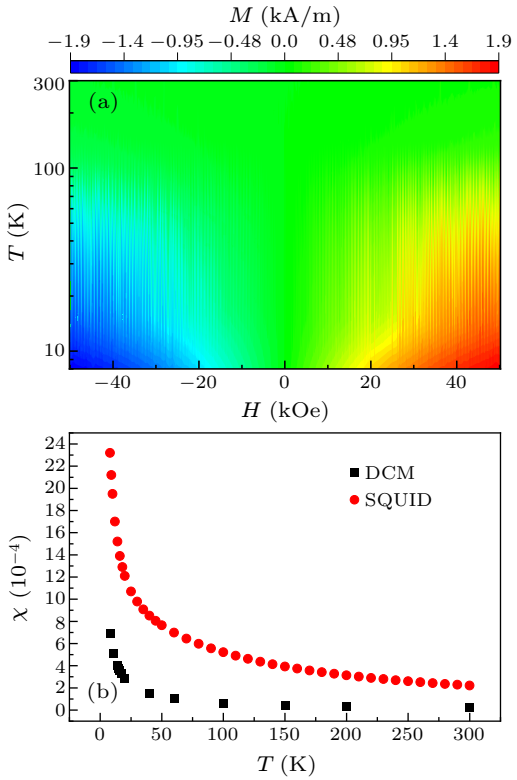

Fig. 5. Quantitative determination of magnetization (a) and susceptibility (b) of the polymer material by dynamic cantilever magnetometry based on our slow relaxation model. The result is consistent with that measured by conventional DC and AC magnetometry, as indicated by the red circle.

In summary, we have proposed a model to explain the $\Delta f \propto H^2$ relationship between dynamic cantilever magnetometry data and extract magnetization and magnetic susceptibility using the experimental data of a cobalt-iridium metal-metalloligand coordination polymer, a paramagnetic material with slow relaxation. A transition of intramolecular coupling at 20 K can be recognized from the second derivative of frequency shift with respect to the field. This work provides a possibility to gain insight into paramagnetic materials, such as magnetization, susceptibility, and relaxation time, using dynamic cantilever magnetometry. Since resonance frequencies of cantilevers range from several Hz to GHz,[32,33] paramagnetic samples with relaxation time ranging from 1 ns to 1 s are possibly studied via dynamic cantilever magnetometry.

Acknowledgments. This work was supported by the National Key Research and Development Program of China (Grant No. 2017YFA0303201), and the National Natural Science Foundation of China (Grant

No. 11704386).

Data Availability. The data that support the findings of this study are available from the corresponding author upon reasonable request.

References

[1] Gysin U, Rast S, Aste A, Speliotis T, Werle C and Meyer E 2011 *Nanotechnology* **22** 285715
[2] Stipe B C, Mamin H J, Stowe T D, Kenny T W and Rugar D 2001 *Phys. Rev. Lett.* **86** 2874
[3] Kamra A, Schreier M, Huebl H and Goennenwein S T B 2014 *Phys. Rev. B* **89** 184406
[4] Yu Y, Xu F, Guo S S, Wang N, Zou L K, Wang B M, Li R W and Xue F 2020 *Appl. Phys. Lett.* **116** 193102
[5] Wang H X, Song J H, Wang W P, Chen Y S, Shen X, Yao Y, Li J J, Sun J R and Yu R C 2021 *Chin. Phys. Lett.* **38** 087502
[6] Na S H, Wu W and Luo J L 2020 *Chin. Phys. Lett.* **37** 087301
[7] Xu F, Guo S S, Yu Y, Wang N, Zou L K, Wang B M, Li R W and Xue F 2019 *Phys. Rev. Appl.* **11** 054007
[8] Overweg H C, den Haan A M J, Eerkens H J, Alkemade P F A, Rooij A L L, Spreeuw R J C, Bossoni L and Oosterkamp T H 2015 *Appl. Phys. Lett.* **107** 072402
[9] Choi H, Kim Y W, Lee S G, Choi M S, Kim M S and Choi J H 2017 *Phys. Rev. B* **95** 064505
[10] Chen L, Yu F, Xiang Z, Asaba T, Tinsman C, Lawson B, Sass P M, Wu W, Kang B L, Chen X and Li L 2018 *Phys. Rev. Appl.* **9** 024005
[11] Li G, Xiang Z, Yu F, Asaba T, Lawson B, Cai P, Tinsman C, Berkley A, Wolgast S, Eo Y S, Kim D J, Kurdak C, Allen J W, Sun K, Chen X H, Wang Y Y, Fisk Z and Li L 2014 *Science* **346** 1208
[12] Moll P J W, Potter A C, Nair N L, Ramshaw B J, Modic K A, Riggs S, Zeng B, Ghimire N J, Bauer E D, Kealhofer R, Ronning F and Analytis J G 2016 *Nat. Commun.* **7** 12492
[13] Modic K A, Bachmann M D, Ramshaw B J, Arnold F, Shirer K R, Estry A, Betts J B, Ghimire N J, Bauer E D, Schmidt M, Baenitz M, Svanidze E, McDonald R D, Shekhter A and Moll P J W 2018 *Nat. Commun.* **9** 3975
[14] Semeghini G, Levine H, Keesling A, Ebadi S, Wang T T, Bluvstein D, Verresen R, Pichler H, Kalinowski M, Samajdar R, Omran A, Sachdev S, Vishwanath A, Greiner M, Vuletić V and Lukin M D 2021 *Science* **374** 1242
[15] Wei Y, Ma X, Feng Z, Zhang Y, Zhang L, Yang H, Qi Y, Meng Z Y, Wang Y C, Shi Y and Li S 2021 *Chin. Phys. Lett.* **38** 097501
[16] Jia Y T, Gong C S, Liu Y X, Zhao J F, Dong C, Dai G Y, Li X D, Lei H C, Yu R Z, Zhang G M and Jin C Q 2020 *Chin. Phys. Lett.* **37** 097404
[17] Leahy I A, Pocs C A, Siegfried P E, Graf D, Do S H, Choi K Y, Normand B and Lee M 2017 *Phys. Rev. Lett.* **118** 187203
[18] Yang C, Wang Z C and Su G 2020 *Chin. Phys. Lett.* **37** 087201
[19] Krivokapic I, Zerara M, Daku M L, Vargas A, Enachescu C, Ambrus C, Tregenna-Piggott P, Amstutz N, Krausz E and Hauser A 2007 *Coord. Chem. Rev.* **251** 364
[20] Shao D, Shi L, Yin L, Wang B L, Wang Z X, Zhang Y Q and Wang X Y 2018 *Chem. Sci.* **9** 7986
[21] Kurmoo M 2009 *Chem. Soc. Rev.* **38** 1353
[22] Xie Z, Ma L, DeKrafft K E, Jin A and Lin W 2010 *J. Am. Chem. Soc.* **132** 922
[23] Greedan J E 2001 *J. Mater. Chem.* **11** 37
[24] Kostakis G E, Perlepesb S P, Blatov V A, Proserpio D M and Powell A K 2012 *Coord. Chem. Rev.* **256** 1246
[25] Perfetti M 2017 *Coord. Chem. Rev.* **348** 171
[26] Fan K, Xu F, Kurmoo M, Huang X D, Liao C H, Bao S S, Xue F and Zheng L M 2020 *Inorg. Chem.* **59** 8935
[27] Weber D P, Rüffer D, Buchter A, Xue F, Russo-Averchi E, Huber R, Berberich P, Arbiol J, Morral A F I, Grundler D and Poggio M 2012 *Nano Lett.* **12** 6139
[28] Gross B, Philipp S, Josten E, Leliaert J, Wetterskog E, Bergström L and Poggio M 2021 *Phys. Rev. B* **103** 014402
[29] Shamsudhin N, Tao Y, Sort J, Jang B, Degen C L, Nelson B J and Pané S 2016 *Small* **12** 6363
[30] Philipp S, Gross B, Reginka M, Merkel M, Claus M M, Sulliger M, Ehresmann A and Poggio M 2021 *Appl. Phys. Lett.* **119** 222406
[31] Binder K and Young A P 1986 *Rev. Mod. Phys.* **58** 801
[32] Gil-Santos E, Ramos D, Martínez J, Fernández-Regúlez M, García R, Paulo S, Calleja M and Tamayo J 2010 *Nat. Nanotechnol.* **5** 641
[33] Nagataki A, Takei K, Arie T and Akita S 2015 *Appl. Phys. Express* **8** 085101